

Submitted to ApJ, June, 1997

A Very Hot, High Redshift Cluster of Galaxies: More Trouble for $\Omega_0 = 1$

Megan Donahue and G. Mark Voit
Space Telescope Science Institute
3700 San Martin Drive
Baltimore, MD 21218
donahue@stsci.edu, voit@stsci.edu

Isabella Gioia^{1,2} and Gerry Luppino²
Institute for Astronomy
2680 Woodlawn Drive
Honolulu, HI 96822
gioia@galileo.ifa.hawaii.edu, ger@galileo.ifa.hawaii.edu

John P. Hughes
Department of Physics and Astronomy
Rutgers University
PO Box 849
Piscataway, NJ 08855-0849
jackph@physics.rutgers.edu

John T. Stocke
University of Colorado
Center for Astrophysics and Space Astronomy
CB 389
Boulder CO 80309
stocke@casa.colorado.edu

¹Home Institution: Istituto di Radioastronomia del CNR, Via Gobetti, 101 40129 Bologna, Italy

²Visiting Astronomer at CFHT, operated by the National Research Council of Canada, le Centre National de la Recherche Scientifique de France and the University of Hawaii, and at the W. M. Keck Observatory, jointly operated by the California Institute of Technology and the University of California.

ABSTRACT

We have observed the most distant ($= 0.829$) cluster of galaxies in the *Einstein* Extended Medium Sensitivity Survey (EMSS), with the ASCA and ROSAT satellites. We find an X-ray temperature of $12.3_{-2.2}^{+3.1}$ keV for this cluster, and the ROSAT map reveals significant substructure. The high temperature of MS1054-0321 is consistent with both its approximate velocity dispersion, based on the redshifts of 12 cluster members we have obtained at the Keck and the Canada-France-Hawaii telescopes, and with its weak lensing signature. The X-ray temperature of this cluster implies a virial mass $\sim 7.4 \times 10^{14} h^{-1} M_{\odot}$, if the mean matter density in the universe equals the critical value ($\Omega_0 = 1$), or larger if $\Omega_0 < 1$. Finding such a hot, massive cluster in the EMSS is extremely improbable if clusters grew from Gaussian perturbations in an $\Omega_0 = 1$ universe. Combining the assumptions that $\Omega_0 = 1$ and that the initial perturbations were Gaussian with the observed X-ray temperature function at low redshift, we show that this probability of this cluster occurring in the volume sampled by the EMSS is less than a few times 10^{-5} . Nor is MS1054-0321 the only hot cluster at high redshift; the only two other $z > 0.5$ EMSS clusters already observed with ASCA also have temperatures exceeding 8 keV. Assuming again that the initial perturbations were Gaussian and $\Omega_0 = 1$, we find that each one is improbable at the $< 10^{-2}$ level. These observations, along with the fact that these luminosities and temperatures of the high- z clusters all agree with the low- z $L_X - T_X$ relation, argue strongly that $\Omega_0 < 1$. Otherwise, the initial perturbations must be non-Gaussian, if these clusters' temperatures do indeed reflect their gravitational potentials.

Subject headings: intergalactic medium – galaxies: clusters: individual (MS1054-0321) – X-rays: galaxies – dark matter – cosmology:observations – galaxies:interactions

1. Introduction

Clusters of galaxies occupy a special position among celestial self-gravitating structures, as they are the largest virialized objects in the universe. If all the cosmic structures we currently see grew hierarchically from small seed perturbations in the early universe, as many lines of evidence now suggest (e.g. Peebles 1993), then the largest clusters of galaxies

are also the most recent virialized structures to have appeared on the cosmological scene. The most massive of all clusters, which represent the most extreme high-density peaks on scales $\sim 10^{15} M_{\odot}$ in the initial field of density perturbations, correspond to several- σ events if the perturbations are Gaussian.

Because massive clusters represent the high- σ tail of the distribution, their number density should rise dramatically as the overall amplitude of the perturbations grows. This characteristic of cluster formation renders massive cluster evolution particularly sensitive to the mean matter density of the universe, currently equal to Ω_0 , in units of the critical density $3H_0^2/8\pi G$. If $\Omega_0 \approx 1$, perturbations should still grow like $(1+z)^{-1}$, and evolution in the number density of distant clusters with redshift should be rapid. If $\Omega_0 \ll 1$, perturbation growth has virtually stopped, and massive cluster evolution should be much more mild.

Evolution in the distribution of cluster masses sensitively indicates Ω_0 , but measuring the virial masses of clusters (M_{vir}) is difficult, even at low redshifts. A much more straightforward observational task is to measure how the X-ray temperatures (T_X) of clusters depend on redshift and then to use a model to relate T_X to M_{vir} (e.g. Oukbir & Blanchard 1992). The *Advanced Satellite for Cosmology and Astrophysics* (ASCA) (Tanaka, Inoue, & Holt 1994) now makes such tests possible because it can measure the temperatures of the most luminous X-ray clusters at high redshifts (Yamashita 1994; Furuzawa et al. 1994; Donahue 1996). Henry (1997) has recently published a temperature function for 10 massive clusters at $z \sim 0.3$, chosen from the *Einstein* Extended Medium Sensitivity Survey (EMSS) (Gioia et al. 1990; Henry et al. 1992). His comparison of the $z \approx 0.3 - 0.4$ temperature function with the $z \approx 0$ temperature function suggests that $\Omega_0 \approx 0.5$ and rules out $\Omega_0 = 1$ with 99% confidence.

In this paper we attempt to extract the maximum leverage out of this test for Ω_0 by measuring the temperature of the highest-redshift cluster in the EMSS, MS1054-0321 at $z = 0.83$. We present both an ASCA spectrum and a ROSAT HRI image of this very luminous cluster ($L_x = 5.6 \times 10^{44} h^{-2} \text{ erg s}^{-1}$ 2-10 keV rest frame, $L_x = 1.1 \times 10^{45} h^{-2} \text{ erg s}^{-1}$ bolometric). For $q_0 = 0.1$, $L_x = 7.7 \times 10^{44} h^{-2} \text{ erg s}^{-1}$ 2-10 keV rest frame. Luppino & Kaiser (1997) provide a true color optical image and a weak lensing map. After presenting the observations in § 2, we examine how they constrain Ω_0 in § 3, finding that they strongly indicate $\Omega_0 < 1$. Section 4 summarizes our results. The ASCA and ROSAT observations we present here are part of a larger program to measure the X-ray temperatures of three high- z , X-ray luminous clusters in the EMSS, the other two being MS0451-03 at $z = 0.53$ (Donahue 1996) and MS1137+66 at $z = 0.78$ (Donahue 1998, in preparation). Throughout the paper, we parametrize $H_0 = 100h \text{ km/sec/Mpc}$ and assume $q_0 = 0.5$, except where noted.

2. Observations and Data Reduction

This section describes the data indicating that MS1054-0321 is an unusually massive cluster. We first discuss the ASCA spectra showing that MS1054-0321 has a temperature in excess of 10 keV. Next we introduce the optical velocity dispersion and lensing data on this cluster, which agree with its high X-ray temperature. Then we show a ROSAT HRI image that reveals substructure in this cluster, suggesting that it may not be fully relaxed.

2.1. ASCA Spectra

ASCA executed a single long ($\sim 70,000$ s) exposure of the cluster MS1054-0321 during May 23-25, 1995. This satellite carries four independent X-ray telescopes, two with Gas Imaging Spectrometers (GIS) and two with Solid-State Imaging Spectrometers (SIS), from which we obtained four independent datasets. The GIS detectors are imaging gas scintillation proportional counters with energy resolutions of 8% at 5.9 KeV and 50' diameter fields of view. The two SIS detectors are X-ray sensitive CCDs with energy resolutions of 2% at 5.9 KeV and 22' by 22' square fields of view. These observations employed the SIS detectors in 2-CCD mode. However, we restricted the data analysis to the CCD containing the target and only used the second CCD to check the background estimates.

To prepare the data for analysis, we extracted clean X-ray event lists using a magnetic cut-off rigidity threshold of 6 GeV c^{-1} and the recommended minimum elevation angles and bright Earth angles to reject background contamination (see Day et al. 1995). Events were extracted from within circular apertures of radii 3.25 arcmin (SIS1), 2.53 arcmin (SIS0), and 5.0 arcmin (GIS) to maximize the ratio of signal to background noise. We rejected $\sim 98\%$ of cosmic ray events by using only SIS chip data grades of 0, 2, 3, 4, and we rejected hot and flickering pixels. Light curves for each instrument were visually inspected, and time intervals with high background or data dropouts were excluded manually. We rebinned the SIS data in the standard way to 512 spectral channels using Bright2Linear (see Day et al. 1995) with the lowest 13 channels flagged as bad, and we regrouped the GIS data so that no energy bin had fewer than 25 counts. Table 1 gives the resulting net count rates and effective exposure times. We do not expect the derived X-ray fluxes to be consistent between the detectors because the target was not centered and some of the extended flux may have missed the SIS detectors.

Background estimates were taken from the regions of the detector surrounding the cluster detection, from summed deep background images supplied by the ASCA Guest

Observer Facility (GOF), and from the second CCD. The deep background spectra were extracted with the same spatial and background removal filters used to extract the source data. The intensities of the local background and the deep background were consistent with each other, but the uncertainties for the deep background estimate were larger (because the source extraction area was smaller). We therefore used the local background estimates for our analysis.

We extracted SIS spectra binned in energy channels in two different ways: (1) binning by a factor 4 in energy, and (2) regrouping the data into energy bins containing a minimum of 16 counts. The first procedure provided slightly better constraints on iron abundance because it maintained some of the spectral resolution around the 6.7 keV Fe line, preserving the predicted contrast between the counts in the energy bin where the line should be and the continuum channels. The second procedure yielded slightly better constraints on temperature. After rebinning the data, we restricted our fitting of the SIS spectra to the 0.5 – 5.5 keV range over which the signal-to-noise was adequate. The adequate range of the GIS spectra extended to 7 keV.

To analyze the spectra, we used XSPEC (v10.0) from the software package XANADU available from the ASCA GOF (Arnaud 1996). We fitted the spectral data from the four ASCA datasets and their respective response files (see Day et al. 1995). The individual SIS response matrices were generated with the tool *sisrmg* (1997 version), which takes into account temporal variations in the gain and removes the inconsistencies seen in data analyzed with the standard SIS response matrices.

The standard model we used to fit the data was a Raymond-Smith thermal plasma with a temperature T_X , absorbed by cold Galactic gas with a characteristic column density of neutral hydrogen N_H . We did not detect a significant intrinsic absorption component, to a 90% upper limit of $N_H < 1.4 \times 10^{21} \text{ cm}^{-2}$. Thus, we fixed soft X-ray absorption at an HI value of $3.7 \times 10^{20} \text{ cm}^{-2}$ (Gioia et al. 1990). Each SIS spectrum was fit with its own normalization; the normalizations of the GIS spectra were constrained to be the same. The parameters varied to provide a fit to 4 spectra were therefore the 3 independent normalizations (1 for each SIS spectrum, 1 for both GIS spectra), a single emission-weighted temperature, and the metallicity (iron abundance). Examples of the binned spectra and best-fit model convolved with each telescope’s response matrix are found in Figure 1. The best-fit redshifted temperature to the binned-by-four spectrum was $12.4 \pm_{2.3}^{3.6} \text{ keV}$ with an upper limit on iron abundance of 0.22 solar, keeping the absorption fixed. If we used the SIS spectra regrouped to a minimum of 16 counts per bin, the best-fit temperature was virtually the same: $12.3 \pm_{2.1}^{3.1} \text{ keV}$ with an upper limit on the iron abundance of < 0.25 solar. All uncertainties quoted are the 90% confidence levels for a 1-dimensional fit ($\Delta\chi^2 = 2.70$),

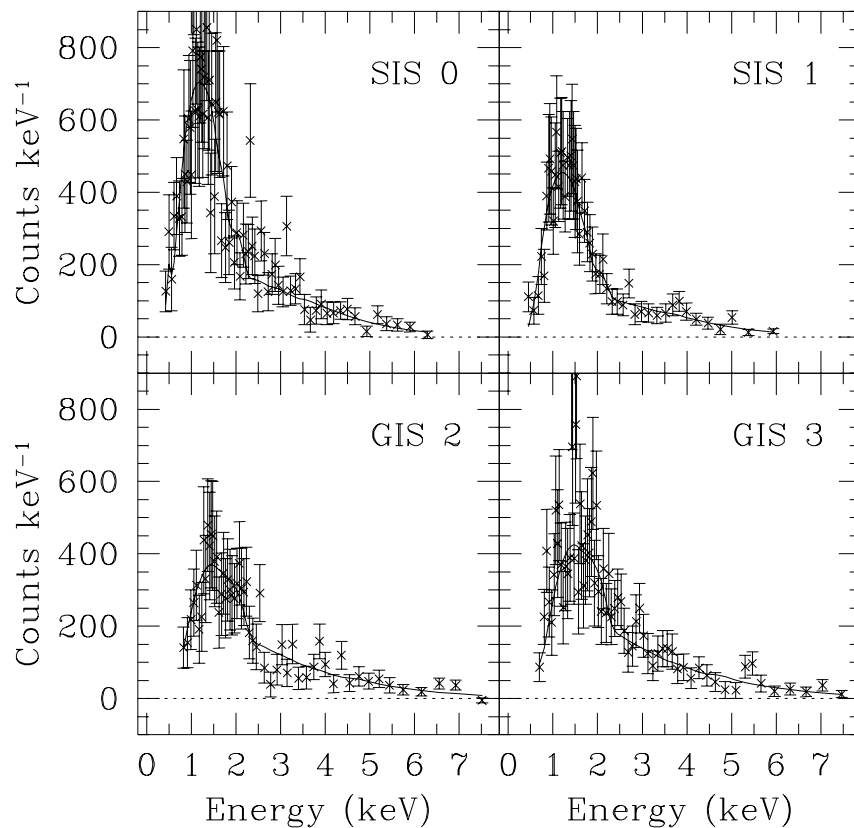


Fig. 1.— We plot the X-ray spectra from each of the four ASCA telescopes for the cluster MS1054-0321. Each spectrum has over 1000 X-ray counts. (See Table 1.) The best-fit model is drawn with a solid line. The spectra we display were binned such that each energy bin contained a minimum of 16 (SIS) or 25 (GIS) counts.

and all fits have an acceptable reduced χ^2 of $\sim 0.8 - 0.9$. Figure 2 shows the two-parameter χ^2 contours for the cluster metallicity and T_X in keV.

2.2. Optical Corroboration

The available optical data on this cluster corroborate the high temperature measured by ASCA. Weak lensing observations of MS1054-0321 by Luppino & Kaiser (1997) show that its mass within $0.5 h^{-1}$ Mpc is $(5 - 11) \times 10^{14} h^{-1}$ Mpc, depending on the redshift distribution of the lensed galaxies. In an isothermal potential, its mass distribution corresponds to an isotropic one-dimensional velocity dispersion $\sim 1100 - 2200 \text{ km s}^{-1}$, consistent with the value expected from the ASCA temperature: $(kT_X/\mu m_p)^{1/2} = 1400 \pm 170 \text{ km s}^{-1}$ (90% confidence limits).

In addition, we have obtained the redshifts of twelve cluster members with the CFHT Multi-Object Spectrograph (MOS) on April 13, 1994 and with the LRIS (Oke et al. 1995) at Keck on January 4, 1995. These are listed in Table 2. Using Timothy Beers' program ROSTAT, we calculated their mean redshift and velocity dispersion, finding $z = 0.829 \pm 0.008$ and a velocity dispersion of $1360 \pm 450 \text{ km s}^{-1}$ (90% confidence interval). (The observed redshift dispersion has been corrected to first order for cosmological redshift by dividing by $1 + z$). Several alternative methods (Beers, Flynn, & Gebhardt 1990) give the same answer within the uncertainties. While the small numbers of redshifts do not constrain the velocity dispersion very well, the value we find is consistent with both the lensing results and the X-ray temperature.

Recent observations of other hot, high- z clusters further support the notion that their temperatures faithfully reflect their gravitational potentials. Figure 3 shows the relationship between the X-ray temperatures and velocity dispersions of three hot X-ray clusters at $z > 0.5$ from the EMSS and two cooler clusters that are companions of MS0016+06 at $z = 0.54$ (Hughes, Birkinshaw, & Huchra 1995; Hughes & Birkinshaw 1998). The X-ray temperatures for the three hot clusters are from this paper, Yamashita (1994), Furuzawa et al. (1994), and Donahue (1996), and their velocity dispersions are from this paper and Carlberg et al. (1996). The data for the two cooler clusters are from Hughes et al. (1995) and Hughes & Birkinshaw (1998). The hotter clusters agree with the relation $kT_X = \mu m_p \sigma_{1D}^2$, while the cooler clusters might be slightly hot for their velocity dispersions, but nevertheless in agreement with the low- z σ - T_X relation of Edge & Stewart (1991a).

Confidence contours

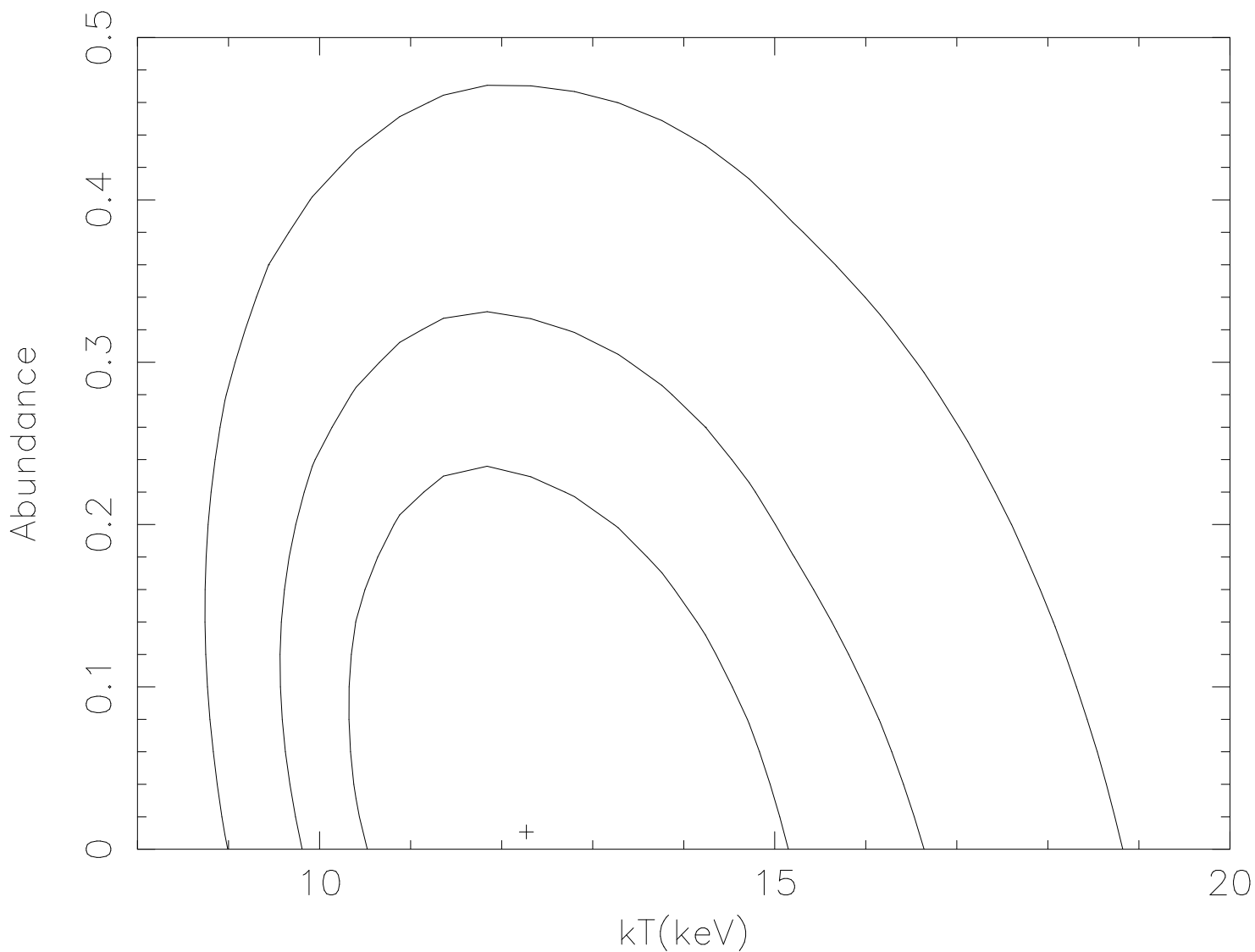


Fig. 2.— We plot the two-dimensional χ^2 contours at 68.3%, 90% and 99% confidence levels ($\Delta\chi^2 = 2.30, 4.61$ and 9.21) for the cluster iron abundance in units of the solar abundance and temperature in keV. These contours represent the confidence contours of simultaneous fits to the SIS spectra and to GIS spectra binned such that each bin contained a minimum of 16 and 25 counts respectively.

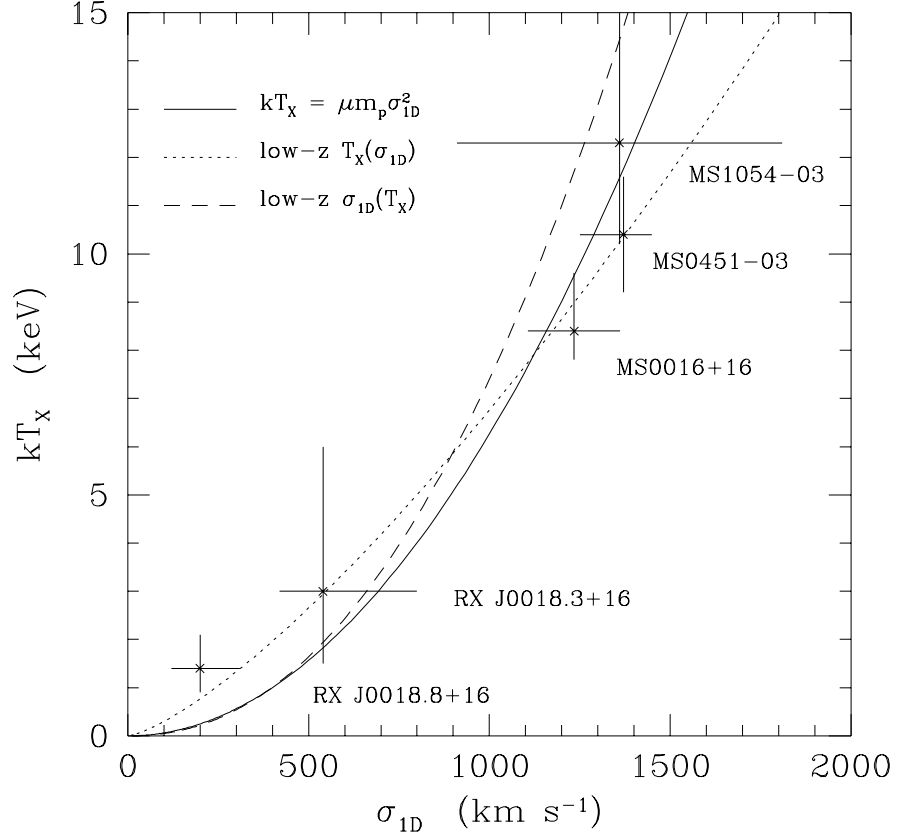


Fig. 3.— The relation between line-of-sight velocity dispersion (σ_{1D}) and X-ray temperature (T_X) for several clusters at $z > 0.5$. The solid lines illustrates the relation $kT_X = \mu m_p \sigma_{1D}^2$, and the other two lines show the σ_{1D} - T_X correlations derived from low- z clusters by Edge & Stewart (1991). The dotted line gives the correlation when T_X is the dependent variable, and the dashed line gives the correlation when σ_{1D} is the dependent variable. Temperatures of high- z clusters at $kT_X \sim 10$ keV appear to indicate the depths of their gravitational potentials with respectable accuracy.

2.3. X-Ray Imaging

Our ROSAT data on this cluster suggest that we ought to interpret its temperature and velocity dispersion cautiously. We observed MS1054-0321 with the ROSAT HRI for over 121,590 seconds on December 6-18, 1996, yielding 1060 ± 90 net counts (including an earlier 12,136 second observation on May 5-6, 1996.) Figure 4 (Plate 1) shows a map of X-ray contours overlaid on a ground-based optical image of the cluster. For this figure, the X-ray emission was smoothed adaptively with Gaussians chosen such that the product of the number of counts and σ^2 was roughly constant. The minimum contour corresponds to 1 count per $8'' \times 8''$, which is $\sim 3 - \sigma$. The cluster emission is clearly extended over a scale of at least one arcminute. With the spatial resolution of the HRI, we have resolved the X-ray emission into two or three clumps and an extended component, clearly indicating that this cluster is not regular.

King models centered on the cD galaxy in MS1054-0321 tend to have high β values ($\beta \sim 0.7 - 1.0$) and large core radii ($\sim 1'$ or $\sim 500h_{50}^{-1}$ kpc), although these values are not well constrained by the HRI data because of the cluster's irregular X-ray shape and clumpiness. A King model is rejected by the data, with reduced $\chi^2 > 2$ for both circular and elliptical King models.

The most western peak is the most significant, containing $\sim 144 \pm 25$ counts within $24''$ above the smooth cluster component. The central peak is smaller, with $\sim 90 \pm 24$ counts and the easternmost peak is the least significant at 44 ± 14 counts above the smooth component. We made a basic statistical test for bimodality of the X-ray distribution of photons with the Lee statistic (Fitchett 1988; Lee 1979). We calibrated the Lee statistic by producing multiple simulations of the null hypothesis in which the cluster emission is distributed in a King model ($\propto (r^2 + r_{core}^2)^{-3\beta+1/2}$) where the core radius is $56''$ and $\beta = 2/3$ or 1. We found that the cluster is at least bimodal at greater than a 99.9% confidence level for either null hypothesis.

The peaks in the X-ray emission do not coincide with any particular optical feature to within the 6 arcsec aspect uncertainty of the X-ray image. The cluster is elongated east-west, in the direction of the galaxy distribution, and a tail extends south of the cluster. Its X-ray emission roughly coincides with the dark matter contours as plotted by Luppino & Kaiser (1997), including the east-west and southerly extensions. The spatial resolution of the weak lensing map is not sufficient to confirm the sub-clumps seen in the X-ray map. The cluster X-ray emission also coincides with the shape of the Sunyaev-Zeldovich temperature decrement detected in centimeter interferometry experiments by L. Grego (PhD thesis, in preparation).

The asymmetric appearance of the cluster in these high resolution images warns us that the relationship between its mass and its temperature might not be as simple as a spherical, hydrostatic, isothermal model would predict. However, recent hydrodynamic simulations of cluster formation beginning with cosmological initial conditions indicate that the systematic errors on cluster masses derived using a scaling relation between mass and temperature are relatively small, typically $< 20\%$ even when some substructure is present (Evrard, Metzler, & Navarro 1996). Higher resolution simulations of individual cluster mergers, whose initial conditions are not dictated by hierarchical structure formation, indicate that errors in the estimated mass can be somewhat larger ($\lesssim 50\%$) after a recent merger, but these errors tend to yield *underestimates* of the cluster’s mass (Roettiger, Burns & Loken 1996; Schindler 1996). The following discussion will therefore focus on the implications of the cluster temperature alone, assuming that the emission-weighted temperature is representative of the virial temperature. Mass errors at the 20% level do not affect the qualitative results of the ensuing discussion.

3. Constraints on Temperature Evolution

This cluster, MS1054-0321, is one of the hottest clusters known. If $\Omega_0 = 1$, structure formation simulations show that we can estimate its virial mass by assuming that the mean density within its virialized region is ~ 200 times the critical density at the cluster’s redshift and that the cluster itself is isothermal (Evrard et al. 1996; Eke et al. 1996). The virial mass of MS1054-0321 would then be approximately $M_{\text{vir}} \sim [2kT_X/\mu m_p(1+z)]^{3/2}(10H_0G)^{-1} \sim 7.4 \times 10^{14} h^{-1} M_\odot$ within $r_{200} = 1.5h^{-1}$ Mpc. (We note that this relation is equivalent to assuming $\beta = 1$ in a standard X-ray mass relation for an isothermal gas.) Such a massive cluster at such a high redshift severely challenges models of hierarchical structure formation with $\Omega_0 = 1$ (Evrard 1989; Peebles, Daly, & Juszkievicz 1989; Donahue 1993). This section elucidates how severe those challenges are.

Because the virial masses of clusters are much harder to measure than their temperatures, we will restrict this analysis to focus on temperature evolution, relying on T_X to be a surrogate for M_{vir} . The analysis will therefore depend on the temperature-mass relation we assume. In an $\Omega_0 = 1$ universe, this relation is relatively simple: $T_X \propto M_{\text{vir}}^{2/3}(1+z)$. If $\Omega_0 \ll 1$, this relationship breaks down below $z \sim \Omega_0^{-1} - 1$ as the development of structure stagnates.

3.1. Rarity of Hot Clusters at High- z

In order to determine the rarity of a cluster as hot as MS1054-0321 in an $\Omega_0 = 1$ universe seeded with Gaussian perturbations, we will assume that the Press-Schechter formula (Press & Schechter 1974) adequately describes the mass function of virialized objects, an assumption borne out by numerical simulations (e.g. Lacey & Cole 1994, Eke et al. 1996). In integral form, the comoving mass density of virialized objects with virial masses greater than M is then

$$\rho(> M) = \rho_0 \operatorname{erfc}(\nu_c/\sqrt{2}) = \frac{2\rho_0}{\sqrt{\pi}} \int_{\nu/\sqrt{2}}^{\infty} e^{-x^2} dx \quad , \quad (1)$$

where ρ_0 is the current mean matter density and ν_c is the critical threshold at which perturbations virialize. This threshold is $\nu_c = \delta_c(t)/\sigma(M)D(t)$, where $\sigma(M)$ describes the rms amplitude of linear perturbations on mass scale M , $D(t)$ describes their linear growth rate, and $\delta_c(t)$ is the linear overdensity at which perturbations virialize. If $\Omega_0 = 1$, then $\nu_c \propto (1+z)$ at a fixed mass scale M .

This integral form of the Press-Schechter formula makes its theoretical underpinnings somewhat more apparent than the more familiar differential form does. The formalism assumes that the original linear density perturbations from which structure grew, smoothed over a length scale corresponding to mass M , follow a gaussian distribution with a dispersion proportional to $\sigma(M)$. As the perturbations grow, the most prominent of them collapse and virialize when their amplitudes exceed some threshold. The parameter ν_c expresses how many standard deviations away from the mean amplitude a positive density perturbation must lie to have collapsed and virialized by time t . The total mass density in virialized perturbations of mass M or greater is then proportional to the integral over the tail of this Gaussian distribution from ν_c to infinity, which yields the complementary error function in the above expression if $\sigma(M) \rightarrow 0$ as $M \rightarrow \infty$. Because the typical amplitudes of perturbations decline with increasing M , the number density of virialized objects exceeding mass M is approximately $M^{-1}\rho(> M)$. At several standard deviations away from the mean, virialized objects with masses significantly exceeding M are much rarer than objects of mass M , so this approximation for the mean number density of virialized clusters is good to a few tens of percent.

We will now proceed to determine the expected number density of clusters like MS1054-0321 at high redshift as follows:

1. We conservatively assume that MS1054-0321 is hotter than 10 keV.
2. In an $\Omega_0 = 1$ universe, $T_X \propto (1+z)$ for clusters of a given mass, so the expected temperature at $z = 0$ of a cluster as massive as MS1054-0321 is > 5.5 keV.

3. Modifying the temperature-mass relation derived from simulations by Evrard et al. (1996) to reflect the mass within a region whose density is 200 times the critical value, we find

$$M_{\text{vir}} \approx (1.8 \times 10^{15} h^{-1} M_{\odot}) \left(\frac{kT_X}{10 \text{ keV}} \right)^{3/2}. \quad (2)$$

This relation yields a virial mass $> 7.4 \times 10^{14} h^{-1} M_{\odot}$ for MS1054-0321.

4. According to Henry (1997) the current number density of clusters hotter than 5.5 keV is $< 3 \times 10^{-7} h^3 \text{ Mpc}^{-3}$. This number density decreases rapidly to higher temperatures and masses, so the mean virialized mass density in clusters hotter than 5.5 keV is $< 2 \times 10^8 h^2 M_{\odot} \text{ Mpc}^{-3}$.
5. Invoking the integral Press-Schechter formula, we find that $\nu_c(z = 0) > 3.4$ for clusters with $T_X > 5.5 \text{ keV}$.
6. Devolving the growth of perturbations back to $z = 0.83$ implies that $\nu_c(z = 0.83) > 6.2$ for clusters with $T_X > 10 \text{ keV}$.
7. At $z = 0.83$, the mean virialized mass density of such clusters in comoving coordinates is thus $< 3.1 \times 10^2 h^2 M_{\odot} \text{ Mpc}^{-3}$, and the corresponding number density is $< 4.4 \times 10^{-13} h^3 \text{ Mpc}^{-3}$.

Next we will show that the detection of MS1054-0321 in the EMSS implies a space density $\sim 10^{-8} h^3 \text{ Mpc}^{-3}$ for like clusters, over 10^4 times what we predict from the current cluster population and the assumption of Gaussian perturbations in an $\Omega_0 = 1$ universe. Before we go on, note that this test for Ω_0 is independent of the mass spectrum of perturbations because we are comparing clusters of similar masses (e.g. Oukbir & Blanchard 1997).

3.2. Hot Clusters in the EMSS

The EMSS is particularly useful for studying cluster evolution because it has a quantifiable selection volume (see Henry et al. 1992; H92 hereafter). The usual procedure for determining the number density of clusters detected in such a survey is to compute V_{max} , the maximum volume within which a cluster of a given flux could be detected, for each cluster. The number density of high-redshift clusters in the survey is then the sum of the $1/V_{\text{max}}$ for all clusters in the redshift shell of interest. Here we consider the $z = 0.5 - 0.9$ shell, which contains 4 EMSS clusters bright enough for ASCA to measure a temperature.

Gioia & Luppino (1994) give the cluster X-ray fluxes within the detection cell for the EMSS clusters at $z > 0.5$. To determine V_{\max} for each cluster, we calculate the maximum redshift z_{\max} at which it could have been detected at each flux limit listed in H92, assuming that the cluster has a core radius of 0.25 Mpc and a β -model surface brightness distribution with $\beta = 2/3$, while correcting for the fraction of the cluster emission that falls into the EMSS detection cell (H92; Donahue, Stocke & Gioia 1991). This correction factor is slightly smaller than two for $z > 0.5$ (H92). We then integrate over $r^2 dr$ with $r = 2cH_0^{-1}[1 - (1 + z)^{-1/2}]$ from the minimum redshift of the shell to either the maximum redshift of the shell or z_{\max} , whichever is smaller. This computation gives the comoving volume per unit steradian associated with the cluster within the specified redshift shell in a flat universe. To determine V_{\max} we multiply this number by the solid angle corresponding to the appropriate flux limit. We compute V_{\max} assuming both (a) no K -correction and (b) a K -correction with $f_\nu \propto \nu^{-0.5}$. Varying any of these assumptions within reasonable ranges changes the results by $\lesssim 10\%$.

The V_{\max} associated with MS1054-0321 in a flat universe is $6.9 \times 10^7 h^{-3} \text{Mpc}^3$ with no K -correction and $6.5 \times 10^7 h^{-3} \text{Mpc}^3$ with the K -correction. These volumes imply a comoving space density $\sim 1.5 \times 10^{-8} h^3 \text{Mpc}^{-3}$ for clusters like MS1054-0321 in the redshift shell $z = 0.5 - 0.9$. Over four orders of magnitude separate this density from the expected value $\sim 4 \times 10^{-13} h^3 \text{Mpc}^{-3}$, casting severe doubts on either the assumption of $\Omega_0 = 1$ or the assumption of Gaussian initial perturbations.

While this single hot high- z cluster argues strongly against $\Omega_0 = 1$, it does not constitute an airtight case on its own. One could argue that MS1054-0321 is anomalous in some way, but there are two other high- z clusters in the EMSS that are nearly as hot: MS0016+16 with $T_X = 8.4 \text{ keV}$ at $z = 0.54$ (Yamashita 1994; Furuzawa et al. 1994) and MS0451-03 with $T_X = 10.4 \pm 1.2 \text{ keV}$ at $z = 0.54$ (Donahue 1996). Figure 3 demonstrates the consistency between their X-ray temperatures and optical velocity dispersions. (MS1137+66, the fourth high redshift EMSS cluster, was observed by ASCA in 1997, and will be discussed in a separate paper.)

For comparison, we can compute the expected number density for these clusters based on the same assumptions as before. Given $T_X > 8 \text{ keV}$ at $z = 0.5$, we find $M_{\text{vir}} > 6.9 \times 10^{14} h^{-1} M_\odot$, corresponding to $T_X > 5.3 \text{ keV}$ at $z = 0$. The current mean virialized mass density in such clusters is similar to the case of MS1054-0321, implying $\nu_c > 3.4$ at $z = 0$ and $\nu_c > 5.2$ at $z = 0.54$. For $\Omega_0 = 1$ and Gaussian perturbations, the expected number density of $> 8 \text{ keV}$ clusters at $z = 0.54$ is then $< 8.6 \times 10^{-11} h^3 \text{Mpc}^{-3}$. Each of the two hot EMSS clusters at $z = 0.54$ would therefore be rarer than one in a hundred, with a joint improbability of order a few times 10^{-4} , somewhat more probable

than the chance occurrence of MS1054-0321.

In summary, given the three hot high redshift clusters in the EMSS, the implied number density of clusters with $T_X > 8$ keV at $z = 0.5 - 0.9$ is $\sim 1.6 \times 10^{-8} h^3 \text{Mpc}^{-3}$. The probability of all three clusters appearing in the volume sampled by the EMSS in an $\Omega = 1$ Universe is $\sim 10^{-6}$ if the initial density perturbations have a Gaussian distribution.

Universes with $\Omega_0 \approx 0.3$ have no problem accomodating such hot clusters at these redshifts. Eke et al. (1996; see also Viana & Liddle 1996) show that the cluster temperature function evolves very little in an $\Omega_0 = 0.3$ universe with no cosmological constant and only modestly in a flat universe with the same Ω_0 . The number density of > 8 keV clusters from Henry (1997) is $\sim 5 \times 10^{-8} h^3 \text{Mpc}^{-3}$, quite close to the value we find at $z \sim 0.5$. The statistics of hot clusters at $z > 0.5$ therefore add substantial weight to the growing body of evidence emerging from cluster evolution that $\Omega_0 \approx 0.3 - 0.5$ (e.g., Carlberg et al. 1997; Henry 1997; Bahcall, Fan, & Cen 1997).

3.3. High- z L_X - T_X Relation

Cluster evolution from $z \sim 0.5$ to the present should be modest at best in a universe with low Ω_0 . Here we show that the relationship between the X-ray luminosity (L_X) and the X-ray temperature of MS1054-0321 is similar to the relationship derived from lower-redshift clusters. Edge & Stewart (1991b) found that $L_X \approx (8.8 \times 10^{41} h^{-2} \text{erg s}^{-1})(T_X/1 \text{keV})^{2.79 \pm 0.05}$ in the 2–10 keV band for low-redshift clusters, while Mushotzky & Scharf (1997) demonstrate that clusters observed at $z > 0.14$ by ASCA, including MS0451-03 (Donahue 1996) and MS0016+16 (Yamashita 1994; Furuzawa et al. 1994), do not deviate appreciably from this relation. Our observations indicate that $L_X(2 - 10 \text{keV}) \approx 7.7 \times 10^{44} h^{-2} \text{erg s}^{-1}$ for MS1054-0321 in its own rest frame ($q_0 = 0.1$), implying an expected temperature of 11.3 keV, on the lower edge of our one-dimensional 90% confidence interval.

The lack of evidence for L_X - T_X evolution in our observation of MS1054-0321 is consistent with the other evidence for $\Omega_0 < 1$, but this test for Ω_0 is not as powerful as the temperature function test, as discussed in Section 3.2. Some cluster evolution models predict little evolution in the L_X - T_X relationship in an $\Omega_0 = 1$ universe, as long as the minimum entropy of the X-ray gas remains the same for all clusters regardless of redshift (Kaiser 1991, Evrard & Henry 1991, Bower 1997). The lack of evolution in L_X - T_X would then require some sort of non-gravitational heating of the X-ray gas.

4. Summary

The ASCA observations we have presented here imply that the EMSS cluster MS1054-0321 at $z = 0.83$ has an X-ray temperature of $12.3_{-2.1}^{+3.1}$ keV. Supporting optical redshifts of 12 member galaxies (this paper) and the weak lensing map (Luppino & Kaiser 1997) provide a velocity dispersion and a lensing mass that agree with the mass inferred from the high X-ray temperature. Our ROSAT image exhibits significant substructure, but numerical modelling of cluster evolution has shown that the presence of substructure does not preclude using a cluster’s X-ray temperature to estimate its virial mass (e.g. Evrard et al. 1996).

This high a temperature in so distant a cluster is powerful evidence that $\Omega_0 < 1$. Using the integral Press-Schechter relation and the current temperature function of clusters, we calculate the expected number density of such hot clusters at $z = 0.83$, under the assumptions of Gaussian perturbations and $\Omega_0 = 1$. We find that the product of the expected number density and the effective volume of the EMSS in the $z = 0.5 - 0.9$ redshift bin is less than a few times 10^{-5} . Similar calculations for two other hot EMSS clusters at $z \approx 0.54$ give probabilities less than a few times 10^{-3} for each one.

For $\Omega_0 \approx 0.3$, the temperature function of hot clusters is expected to evolve very little to redshifts > 0.5 (Eke et al. 1996), so that the hot EMSS clusters are quite consistent with a low- Ω_0 universe. We also find that MS1054-0321 luminosity and temperature are consistent with the low- z L_X - T_X relation, a result also consistent with $\Omega_0 < 1$. These results strongly support the mounting body of evidence (e.g. Carlberg et al. 1997) showing that the mean density of matter in the universe is $\Omega_0 \approx 0.3$.

MD acknowledges Timothy Beers for the use of his ROSTAT program to calculate velocity dispersions, and helpful discussions with Carlos Frenk and Bharat Ratra at the Aspen Center for Physics. This work was supported by NASA ROSAT grant NAG5-2021, NASA ASCA grant NAG5-2570. IMG acknowledges partial support from NASA STScI grant GO-542.01-93A and ASI94-RS-10. IMG acknowledges support from NSF AST95-00515. JPH’s research on clusters is supported by NASA Long Term Space Astrophysics Grant NAG5-3432. MD acknowledges Paul Lee for assistance with ASCA data extraction.

REFERENCES

- Arnaud, K. A. 1996, *Astronomical Data Analysis Software and Systems V*, eds. G. Jacoby and J. Barnes, ASP Conf. Series vol 101.
- Bahcall, N. A., Fan, X., & Cen, R. 1997, *ApJ*, 490, L123.
- Beers, T.C., Flynn, K., & Gebhardt, K. 1990, *AJ*, 100, 32.
- Bower, R. G. 1997, *MNRAS*, 288, 355
- Carlberg, R. G., Morris, S. L., Yee, H. K. C., & Ellingson, E. 1997, *ApJ*, 479, L19.
- Carlberg, R. G., Yee, H. K. C., Ellingson, E., Abraham, R., Gravel, P., Morris, S., & Pritchett, C. J. 1996, *ApJ*, 462, 32
- Day, C., Arnaud, K., Ebisawa, K., Gotthelf, E., Ingham, J., Mukai, K., & White, N. 1995, “The ABC Guide to ASCA Data Reduction, Fourth Version”, available by request from the ASCA GOF.
- Donahue, M. 1993 in *Evolution of Galaxies and Their Environment*, (Kluwer: Dordrecht), eds. J. M. Shull & H. A. Thronson, Jr., p. 409.
- Donahue, M. 1996, *ApJ*, 468, 79.
- Donahue, M., Stocke, J. T., & Gioia, I. M. 1991, *ApJ*, 385, 49.
- Edge, A. C. & Stewart, G. C. 1991a, *MNRAS*, 252, 428.
- Edge, A. C., & Stewart, G. C. 1991b, *MNRAS*, 252, 414
- Eke, V. R., Cole, S., & Frenk, C. S. 1996, *MNRAS*, 282, 263.
- Evrard, A. E. 1989, *ApJ*, 341, L71
- Evrard, A. E. & Henry, J. P. 1991, *ApJ*, 383, 95.
- Evrard, A. E., Metzler, C. A. & Navarro, J. F. 1996, *ApJ*, 469, 494.
- Fitchett, M. 1988, *MNRAS*, 230, 161.
- Furuzawa, A., Yamashita, K., Tawara, Y., Tanaka, Y., & Sonobe, T. 1994, in *New Horizon of X-ray Astronomy*, eds. F. Makino and T. Ohashi, (Universal Academy Press: Tokyo), p. 541.
- Gioia, I. M., Maccacaro, T., Schild, R. E., Wolter, A., Stocke, J. T. 1990, *ApJS*, 72, 567.
- Gioia, I. M. & Luppino, G. A. 1994, *ApJS*, 94, 583.
- Henry, J. P., Gioia, I. M., Maccacaro, T., Morris, S. L., Stocke, J. T. 1992, *ApJ*, 386, 408. (H92).
- Henry, J. P. 1997, *ApJ*, 489, L1

- Hughes, J. P., & Birkinshaw, M. 1998, ApJ, in press (astro-ph/9711203)
- Hughes, J. P., Birkinshaw, M., & Huchra, J. P. 1995, ApJ, 448, L93
- Kaiser, N. 1991, ApJ, 383, 104.
- Lacey, C., & Cole, S. 1994, MNRAS, 271, 676
- Lee, K. L. 1979, J. Am. Statistical Ass., 74, 708.
- Luppino, G. A. & Kaiser, N. 1997, ApJ, 475, 20.
- Mushotzky, R. & Scharf, C. A. 1997, ApJ, 482, L13.
- Oke, J.B., Cohen, J.G., Carr, M., Cromer, J., Dingizian, A., Harris, F.H., Labrecque, S., Luciano, R., Schaal, W., Epps, H., & Miller, J., 1995, PASP, 107, 375.
- Oukbir, J. & Blanchard, A. 1992, A&A, 262, L21.
- Oukbir, J. & Blanchard, A. 1997, A&A, 317, 1.
- Peebles, P. J. E. 1993, Principles of Physical Cosmology, Princeton: Princeton University Press, p. 98.
- Peebles, P. J. E., Daly, R., & Juszkeiewicz, R. 1989, ApJ, 347, 563
- Press, W. & Schechter, P. 1974, ApJ, 187, 425.
- Roettiger, K., Burns, J. O., & Loken, C. 1996, ApJ, 473, 651.
- Schindler, S. 1996, A&A, 305, 756.
- Tanaka, Y., Inoue, H., & Holt, S. S. 1994, PASJ, 46, L37.
- Viana, P. T. P. & Liddle, A. R. 1996, MNRAS, 281, 323.
- Yamashita, K. 1994, in New Horizon of X-ray Astronomy, eds. F. Makino and T. Ohashi, (Universal Academy Press: Tokyo), p. 279.

Table 1: ASCA Observing Information

Detector	Aperture Radius Arcmin	Count Rates s^{-1}	Useful Exposure Time s
SIS0	2.53	0.019	62,019
SIS1	3.25	0.013	58,176
GIS2	5.00	0.012	65,534
GIS3	5.00	0.016	65,920

Table 2: Member Galaxy Redshifts

ID	Redshift	Offset E/W (+/-")	Offset N/S (+/-")
1 (cD)	0.8309 ± 0.0008	0.0	0.0
2	0.8342 ± 0.003	+23	-6
3	0.8127 ± 0.0003	+56	-5.5
4	0.8213 ± 0.0007	+37	+30
5	0.830 ± 0.008	-14	-20
6	0.8209 ± 0.001	-29	-13
7	0.8286 ± 0.001	-31.5	-11.5
8	0.8353 ± 0.0006	-38	-8
9	0.8332 ± 0.001	-43	-6
10	0.8143 ± 0.002	-38	+0.5
11	0.8378 ± 0.003	-80	-44
12	0.8319 ± 0.002	-97.5	-38.5

Fig. 4.— Plate 1. The central $3.75' \times 3.75'$ of the cluster MS1054-0321. The optical image is a 14,400 second I-band image taken with the University of Hawaii 88-inch (Gioia & Luppino 1994). The ROSAT HRI image, a sum of all available HRI data for a total livetime of 121,590 seconds, was rebinned into $8'' \times 8''$ pixels and adaptively smoothed with three Gaussians with sigmas of 16, 14.3, and 12.6 arcseconds corresponding to counts in a pixel of < 10 , $10 - 13.5$ and > 13.5 . The sigmas were chosen so that the products of the number of counts and σ^2 were roughly constant. The background was 9.4164 counts per pixel. The net contour levels are 1, 2.8, 4.6, 6.4, 8.2, and 10 counts per pixel. These net count rates correspond to X-ray surface brightnesses of 1.4, 3.9, 11.6, and 14.0×10^{-14} erg cm $^{-2}$ s $^{-1}$ arcmin $^{-2}$ assuming that 1 HRI count $\sim 2.8 \times 10^{-11}$ erg cm $^{-2}$. The galaxies are marked with identifications corresponding to Table 2. The central galaxy is at RA(2000)=10 56 59.9 and Dec(2000)=03 37 37.3, as measured from our HST image of this cluster (Donahue et al., in preparation).

